

Does a generalized Chaplygin gas correctly describe the cosmological dark sector?

R.F. vom Marttens^{*},¹ L. Casarini [†],^{1,2}

W. Zimdahl[‡],¹ W.S. Hipólito-Ricaldi[§],³ and D.F. Mota[¶]²

¹*Universidade Federal do Espírito Santo, Departamento de Física*

*Av. Fernando Ferrari, 514, Campus de Goiabeiras,
CEP 29075-910, Vitória, Espírito Santo, Brazil*

²*Institute of Theoretical Astrophysics,
University of Oslo, 0315 Oslo, Norway*

³*Universidade Federal do Espírito Santo,
Departamento de Ciências Naturais*

Rodovia BR 101 Norte, km. 60, CEP 29932-540, São Mateus, Espírito Santo, Brazil

(Dated: February 3, 2017)

Abstract

Yes, but only for a parameter value that makes it almost coincide with the standard model. We reconsider the cosmological dynamics of a generalized Chaplygin gas (gCg) which is split into a cold dark matter (CDM) part and a dark energy (DE) component with constant equation of state. This model, which implies a specific interaction between CDM and DE, has a Λ CDM limit and provides the basis for studying deviations from the latter. Including matter and radiation, we use the (modified) CLASS code [1] to construct the CMB and matter power spectra in order to search for a gCg-based concordance model that is in agreement with the SNIa data from the JLA sample and with recent Planck data. The results reveal that the gCg parameter α is restricted to $|\alpha| \lesssim 0.05$, i.e., to values very close to the Λ CDM limit $\alpha = 0$. This excludes, in particular, models in which DE decays linearly with the Hubble rate.

PACS numbers:

^{*} E-mail: rodrigovonmarttens@gmail.com

[†] E-mail: casarini.astro@gmail.com

[‡] E-mail: winfried.zimdahl@pq.cnpq.br

[§] E-mail: wiliam.ricaldi@ufes.br

[¶] E-mail: d.f.mota@astro.uio.no

I. INTRODUCTION

A large part of the current cosmological literature is devoted both to a theoretical understanding of the Λ CDM model and to its observational verification. While it has become the status of a standard model it relies on the assumption of a dark sector which is far from being understood physically. Given its simplicity, it is considered very successful observationally, no competing model is doing better at the moment, but there remain also tensions [2]. It is of ongoing interest therefore to check the status of the Λ CDM model by modifying its basic assumption and to test the observational consequences of such modifications.

One line of research that has been followed in this context relies on the dynamics of Chaplygin gases [3]. The Chaplygin gas in its original form, characterized by an equation of state (EoS) $p = -\frac{A}{\rho}$, was applied to cosmology in [4] followed by [5, 6]. Here, A is a strictly positive constant, p is the pressure and ρ is the energy density. Its relation to higher-dimensional theories was pointed out in [7]. A phenomenological generalization to an EoS

$$p = -\frac{A}{\rho^\alpha}, \quad (1)$$

with a constant $\alpha > -1$ was introduced in [8], where also its relation to a scalar-field Lagrangian of a generalized Born-Infeld type was clarified. For $\alpha = 1$ the original Chaplygin gas is recovered, the case $\alpha = 0$ is related to the Λ CDM model. A Chaplygin gas has the appealing feature that it allows for a unified description of the dark sector. Its energy density changes smoothly from that of nonrelativistic matter at early times to an almost constant value in the far future. Thus it may interpolate between an early phase of decelerated expansion, necessary for structure formation to occur, and a later period in which this substratum acts similarly as a cosmological constant, giving rise to an accelerated expansion. While the mentioned unifying aspects seem to offer a conceptual advantage compared with other approaches, one faces the problem that a successful description of structure formation requires a separation of the observable pressureless matter component. At first sight this seems to be a step back. However, since for the gCg the total energy density is analytically known it is possible to identify the coupling of this separated matter part to the remaining part that plays the role of DE and completes the overall Chaplygin gas. Cosmological models based on the dynamics of generalized Chaplygin gases have attracted considerable interest [9–20]. But this type of models had temporarily been seen as disfavored since in their adiabatic ver-

sion they predict unobserved oscillations and/or instabilities in the matter power spectrum [12]. It turned out, however, that nonadiabatic perturbations may remove such unwanted features [14–16]. Generalized Chaplygin gas models share similarities with decaying vacuum models (see, e.g., [21–29]) which result as special cases if the constant EoS parameter of the DE component is chosen to be -1 .

The aim of this paper which extends and completes previous studies of related configurations [30–32], is to carefully reconsider cosmological models in which CDM and DE combine to behave as a gCg, modeling the dark sector of the Universe. We shall consider the cosmic substratum as built of this dark sector together with baryons and radiation. Starting point of the numerical part is a confrontation of the background dynamics with the JLA sample of supernovae of type Ia [33]. The parameter α which represents a measure of the distance to the Λ CDM model is poorly constrained by the SNIa data. However, the analysis of the JLA sample provides us with a range of values for the present dark matter fraction Ω_{c0} for any admissible α . This information is then used to calculate the CMB and the matter power spectra with the help of the CLASS code [1]. The observed CMB spectrum puts strong limits on α which is restricted to values very close to the Λ CDM limit $\alpha = 0$. These limits are consistent with those obtained by a comparison of the gCg based matter power spectrum with its Λ CDM counterpart.

The structure of the paper is as follows. In section II we recall basic relations for the gCg and introduce its decomposition into an interacting system of nonrelativistic matter and a DE component with constant EoS parameter. On this basis we establish, in section III, a cosmological four-component model by adding baryons and radiation. In section IV the background dynamics is confronted with SNIa data from the JLA sample. This analysis is also used in section V to test the validity of an approximate analytic solution for the Hubble rate of the four-component system. Section VI is devoted to the system of first-order perturbation equations and provides the basis for the application of the CLASS code in section VII. Our results are summarized in section VIII.

II. GENERALIZED CHAPLYGIN GAS

We start by modeling the cosmic medium as a one-component gCg with a variable EoS parameter (cf. (1))

$$w = \frac{p}{\rho} = -\frac{A}{\rho^{\alpha+1}}, \quad (-1 \leq w < 0), \quad (2)$$

which enters the energy conservation equation,

$$\dot{\rho} + 3H(1+w)\rho = 0. \quad (3)$$

A dot denotes the derivative with respect to cosmic time, a is the scale factor of the Robertson-Walker metric and $H = \frac{\dot{a}}{a}$ is the Hubble parameter. The solution of the continuity equation (3) is

$$\rho = \left[A + \frac{(1-A)}{a^{-3(1+\alpha)}} \right]^{\frac{1}{1+\alpha}}. \quad (4)$$

The present value of the scale factor was taken to be $a_0 = 1$. This solution represents a unification of the dark sector in the sense that it behaves as matter, $\rho \propto a^{-3}$ for $a \ll 1$ and $\rho \approx \text{constant}$ for $a \gg 1$.

Considering a spatially flat universe, the system dynamics is given by Friedmann's equation

$$3H^2 = 8\pi G\rho \quad (5)$$

and by

$$\dot{H} = -4\pi G(\rho + p). \quad (6)$$

The gCg is now split into a pressureless component, denoted by a subindex c , which is identified with CDM, and a remaining part, denoted by a subindex Λ , which is supposed to represent a form of DE, characterized by an EoS $p_\Lambda = w_\Lambda \rho_\Lambda$ with a generally time-varying EoS parameter w_Λ ,

$$\rho = \rho_c + \rho_\Lambda, \quad p = p_c + p_\Lambda = p_\Lambda = w_\Lambda \rho_\Lambda. \quad (7)$$

The total pressure of the fluid is due the DE pressure. For a semi-analytic treatment an explicit dependence $w_\Lambda(a)$ is required. We shall restrict ourselves in the following to a constant w_Λ . Later on we shall focus on the case $w_\Lambda = -1$ which is usually associated with a

time-varying vacuum energy. Then, using the Friedmann equation (5), one has

$$\rho_\Lambda = \frac{w}{w_\Lambda} \frac{3H^2}{8\pi G} = \rho_{\Lambda 0} \left(\frac{H}{H_0} \right)^{-2\alpha}. \quad (8)$$

For the special case $w_\Lambda = -1$ we recover the corresponding relation of [18]. With $w_\Lambda = -1$ and $\alpha = 0$ the Λ CDM model is reproduced. The decaying vacuum model of [28] corresponds to $w_\Lambda = -1$ and $\alpha = -\frac{1}{2}$.

The separation of the gCg into two components is accompanied by an interaction between them. With (8) and assuming

$$\dot{\rho}_\Lambda + 3H(1 + w_\Lambda)\rho_\Lambda = Q, \quad (9)$$

$$\dot{\rho}_c + 3H\rho_c = -Q, \quad (10)$$

the source (loss) term Q is found to be

$$Q = 3H[\alpha(1 + w) + 1 + w_\Lambda]\rho_\Lambda. \quad (11)$$

Notice that the term in the square brackets is not constant. It approaches a constant value only in the high-redshift limit $w \ll 1$. It is only in this limit that the frequently used dependence $Q \propto H\rho_\Lambda$ (see, e.g. [34–37]) is approximately valid. If $Q > 0$ the CDM component decays into DE, if $Q < 0$ the DE component decays into CDM. The sign is determined by the interplay between α and w_Λ in the square bracket of (11). Since $w \geq -1$, the direction of the energy flux is defined by the sign of α for $w_\Lambda = -1$. For $\alpha = 0$ and $w_\Lambda = -1$ the interaction vanishes and we consistently recover the Λ CDM model. Note that if only $\alpha = 0$ we do not recover the w CDM model, but we have a coupling that is proportional to $1 + w_\Lambda$.

The interaction term (11) may be rewritten as

$$Q = 3H \left[\alpha \frac{\rho_c \rho_\Lambda}{\rho} + (1 + w_\Lambda) \left(\alpha \frac{\rho_\Lambda}{\rho} + 1 \right) \rho_\Lambda \right]. \quad (12)$$

For $w_\Lambda = -1$ the second term in the square bracket does not contribute. For this special case the interaction assumes a nonlinear structure similar to the cases studied in [31, 32, 38, 39]. In the following section we extend this simplified model to include baryons and radiation.

III. GCG BASED COSMOLOGICAL MODEL

From now on we consider a universe composed of four components described as perfect fluids: radiation (subindex r), baryonic matter (subindex b), CDM, (subindex c) and DE

(subindex Λ),

$$\rho = \rho_c + \rho_\Lambda + \rho_r + \rho_b, \quad p = p_\Lambda + p_r. \quad (13)$$

Because of the radiation component equation (8) is no longer exactly valid in our four-component system. But we continue to use it as an *ansatz*. Radiation and baryonic matter will be treated as separately conserved components.

Our model faces the problem that in the presence of radiation the Hubble rate is no longer analytically known. Introducing the dimensionless quantity E by

$$H(a) \equiv H_0 E(a), \quad (14)$$

as well as

$$\Omega_{\Lambda 0} = \frac{8\pi G \rho_{\Lambda 0}}{3H_0^2}, \quad \Omega_{r0} = \frac{8\pi G \rho_{r0}}{3H_0^2}, \quad (15)$$

use of (5), (6) and (8) provides us with the following differential equation for the Hubble rate:

$$2 \frac{dE}{da} E a = -3E^2 - 3w_\Lambda \Omega_{\Lambda 0} E^{-2\alpha} - \Omega_{r0} a^{-4}. \quad (16)$$

For a negligible radiation component equation (16) has the analytical solution

$$H = H_0 \left\{ -w_\Lambda (1 - \Omega_{m0}) + [1 + w_\Lambda (1 - \Omega_{m0})] a^{-3(1+\alpha)} \right\}^{\frac{1}{2(1+\alpha)}}, \quad (\Omega_{r0} = 0), \quad (17)$$

where

$$\Omega_{c0} = \frac{8\pi G \rho_{c0}}{3H_0^2}, \quad \Omega_{b0} = \frac{8\pi G \rho_{b0}}{3H_0^2}, \quad \Omega_{m0} = \Omega_{c0} + \Omega_{b0}. \quad (18)$$

Such solution, for $\alpha = -0.5$, has been used for a SNe Ia analysis in [40]). However, at high redshift the radiation component plays an important role. To take into account the radiation component properly, we use the analytical approximation

$$H = H_0 \sqrt{[-w_\Lambda (1 - \Omega_{m0}) + [1 + w_\Lambda (1 - \Omega_{m0})] a^{-3(1+\alpha)}]^{\frac{1}{1+\alpha}} + \Omega_{r0} a^{-4}}. \quad (19)$$

This expression is obtained by adding a radiation contribution in (17). The viability of this approximation will be tested below. Note that in equation (19) the terms Ω_{m0} and w_Λ only appear in the combination $w_\Lambda (1 - \Omega_{m0})$. This means, Ω_{m0} and w_Λ are not separate degrees of freedom here. Therefore it is useful to define a variable $\tilde{\Omega}_{m0}$ by

$$1 - \tilde{\Omega}_{m0} = -w_\Lambda (1 - \Omega_{m0}). \quad (20)$$

This degeneracy, which is not a consequence of our approximation, means that any cosmological test which relies on the Hubble rate cannot constrain w_Λ and Ω_{c0} (or equivalently $\Omega_{\Lambda0}$) at the same time. For $w_\Lambda = -1$ the parameters $\tilde{\Omega}_{m0}$ and Ω_{m0} coincide. In terms of $\tilde{\Omega}_{m0}$ the Hubble rate (19) can then be written as

$$H = H_0 \sqrt{\left(1 - \tilde{\Omega}_{m0} + \tilde{\Omega}_{m0} a^{-3(1+\alpha)}\right)^{\frac{1}{1+\alpha}} + \Omega_{r0} a^{-4}}. \quad (21)$$

Using this approximate solution in (8), the DE energy density becomes

$$\rho_\Lambda = \frac{3H_0^2}{8\pi G} \Omega_{\Lambda0} \left[\left(1 - \tilde{\Omega}_{m0} + \tilde{\Omega}_{m0} a^{-3(1+\alpha)}\right)^{\frac{1}{1+\alpha}} + \Omega_{r0} a^{-4} \right]^{-\alpha}, \quad (22)$$

where $\Omega_{\Lambda0} = 1 - \Omega_{m0} - \Omega_{r0}$. The CDM energy density is found through

$$\rho_c = \frac{3H^2}{8\pi G} - \rho_\Lambda - \rho_b - \rho_r, \quad (23)$$

where ρ_b and ρ_r are given by

$$\rho_b = \frac{3H_0^2}{8\pi G} \Omega_{b0} a^{-3}, \quad (24)$$

and

$$\rho_r = \frac{3H_0^2}{8\pi G} \Omega_{r0} a^{-4}, \quad (25)$$

respectively. In the following section we confront this background dynamics with the binned SNIa data from the JLA sample [33]. Since even the most distant supernovae have a low redshift (compared with the redshift of the last-scattering surface), the radiation component in the energy balance is small and the approximate solution is justified for this analysis.

IV. SUPERNOVAE STATISTICAL ANALYSIS

The baryon-photon subsystem of the cosmic medium will be treated here in the same manner as it is treated in the Λ CDM model. We fix Ω_{b0} and Ω_{r0} according to their best-fit values in [41]. We divide our analysis into two parts. At first we consider the dynamics for $w_\Lambda = -1$ with the three free parameters Ω_{c0} , h and α , where h is introduced as usual by $H_0 = 100h \text{ kms}^{-1}\text{Mpc}^{-1}$. In the second part we deal with the general case $w_\Lambda \neq -1$ with the free parameters $\tilde{\Omega}_{m0}$, h and α . In the general case we use equation (21) for the Hubble rate, while for $w_\Lambda = -1$ we have the explicit expression

$$H = H_0 \sqrt{\left[1 - (\Omega_{c0} + \Omega_{b0}) + (\Omega_{c0} + \Omega_{b0}) a^{-3(1+\alpha)}\right]^{\frac{1}{1+\alpha}} + \Omega_{r0} a^{-4}} \quad (w_\Lambda = -1). \quad (26)$$

The results for the time varying vacuum model ($w_\Lambda = -1$) will be used to establish a 2σ range of admissible values for each of the free parameters. Posteriorly, in order to obtain the CMB power spectrum, we use this range as a *prior* to compare the approximate solution of the Hubble rate (26) against the numerical solution of the differential equation (16) with $w_\Lambda = -1$. A similar analysis for a general EoS will be used to constrain Ω_{c0} and w_Λ .

As is well known, SNe Ia tests are using the luminosity distance modulus (the superscript “th” means “theoretical”),

$$\mu^{th} = 5 \log [d_L(z)] + \mu_0, \quad (27)$$

with $\mu_0 = 42.384 - 5 \log(h)$, where

$$d_L(z) = (z+1) H_0 \int_0^z \frac{d\tilde{z}}{H(\tilde{z})} \quad (28)$$

is the luminosity distance. The crucial quantity for the statistical analysis is

$$\chi_{SN}^2 = \Delta\mu^T(\theta) \mathcal{C} \Delta\mu(\theta). \quad (29)$$

Here, \mathcal{C} denotes the covariance matrix and $\Delta\mu$ is a vector whose i -th component is given by $\Delta\mu_i = \mu_i^{obs} - \mu^{th}(z_i)$, where the observational distance modulus μ^{obs} has the structure [33]

$$\mu^{obs} = m_M^* - (M_B - \alpha X_1 + \beta C). \quad (30)$$

The quantities α (here *not* the gCg parameter), β and M_B are nuisance parameters and m_M^* , X_1 and C are light-curve parameters. Since the model has an isotropic luminosity distance, it is possible to use the 31 binned data and the corresponding covariance matrix of [33]. In TABLE I we present the 2σ confidence level constraints of this analysis for the case $w_\Lambda = -1$. The resulting distance modulus for the best-fit values of TABLE I is visualized and compared with the Λ CDM values in FIG. 1. The scale-factor dependences of the fractional abundances of the components and of the Hubble rate are displayed by FIG. 2. For comparison we include also the Λ CDM results. One expects that differences in those background quantities which appear as coefficients in the perturbation equations will also affect the CMB spectrum.

FIG. 3 shows the marginalized 1σ and 2σ contours and the probability distribution functions (PDFs) for each of the free parameters. Note that the SNe Ia analysis does not impose strong constraints on the gCg parameter α . Both $\alpha = 0$ and $\alpha = -1$ are within the 2σ confidence region.

For the general case the SNe Ia statistical analysis provides us with $\tilde{\Omega}_{m0} = 0.363 \pm_{0.145}^{0.075}$. Using this result together with equation (20) we may infer a range of admissible combinations

TABLE I: Result of SNe Ia statistical analysis for the time varying vacuum model ($w_\Lambda = -1$).

Ω_{c0}	h	α
$0.317 \pm_{0.144}^{0.078}$	$0.697 \pm_{0.012}^{0.019}$	$-0.528 \pm_{0.540}^{0.729}$

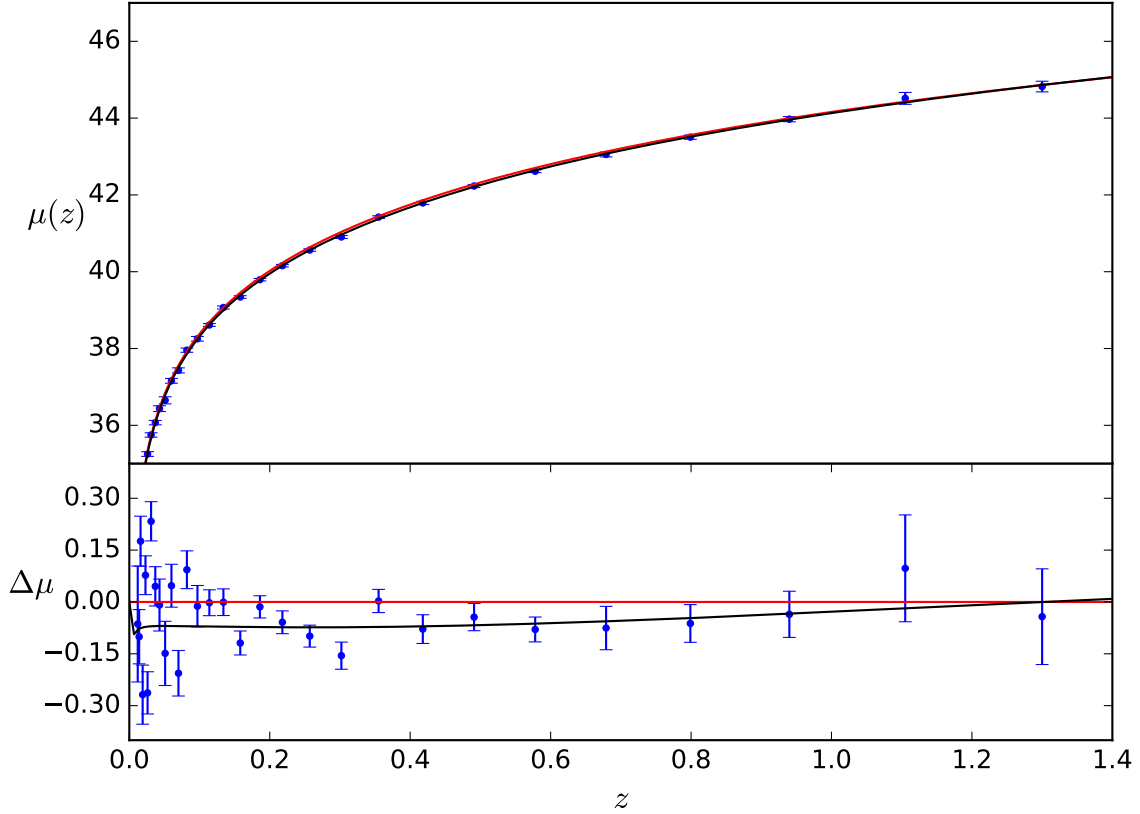


FIG. 1: Upper part: distance modulus calculated from Eq. (27) with the best-fit values of TABLE I (black curve). The red curve represents the Λ CDM model with the best-fit values of [33]. Lower part: difference $\Delta\mu$ between the distance modulus of our model and the distance modulus of the Λ CDM model.

of Ω_{m0} and w_Λ . FIG. 4 shows the allowed region in the $w_\Lambda - \Omega_{m0}$ plane. Since Ω_{c0} and w_Λ are only weakly constrained separately by this analysis, we focus on the vacuum model $w_\Lambda = -1$ in the following.

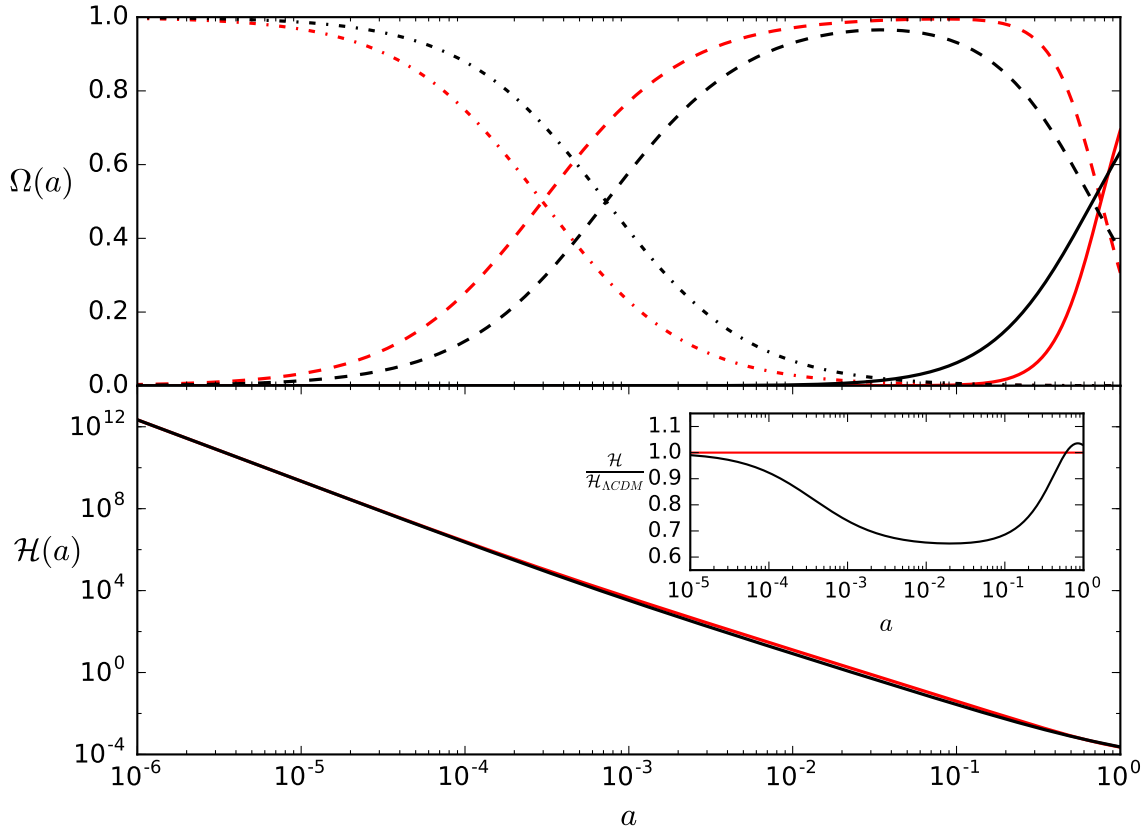


FIG. 2: Upper part: fractional abundances of the components. The dot-dashed lines describe the radiation fractions, the dashed lines the matter fractions and the solid lines the DE fractions (black for our model, red for Λ CDM). Lower part: Hubble rate for the present model compared with that for the Λ CDM model.

V. APPROXIMATE SOLUTION FOR THE HUBBLE RATE

For the SNIa analysis of the previous section the rôle of the radiation component was marginal. For a study of the CMB anisotropy spectrum its appropriate inclusion is essential, however. This raises the question of whether the expression (26) is a good approximation to the exact solution of the differential equation (16) for $w_\Lambda = -1$. Since we prefer to work with an analytic solution we shall test its viability by comparing it with the numerical solution of (16). To this purpose we define the deviation between the approximate analytic and the numerical solutions by

$$\text{Deviation} = \frac{H_{\text{num.}} - H_{\text{approx.}}}{H_{\text{num.}}}. \quad (31)$$

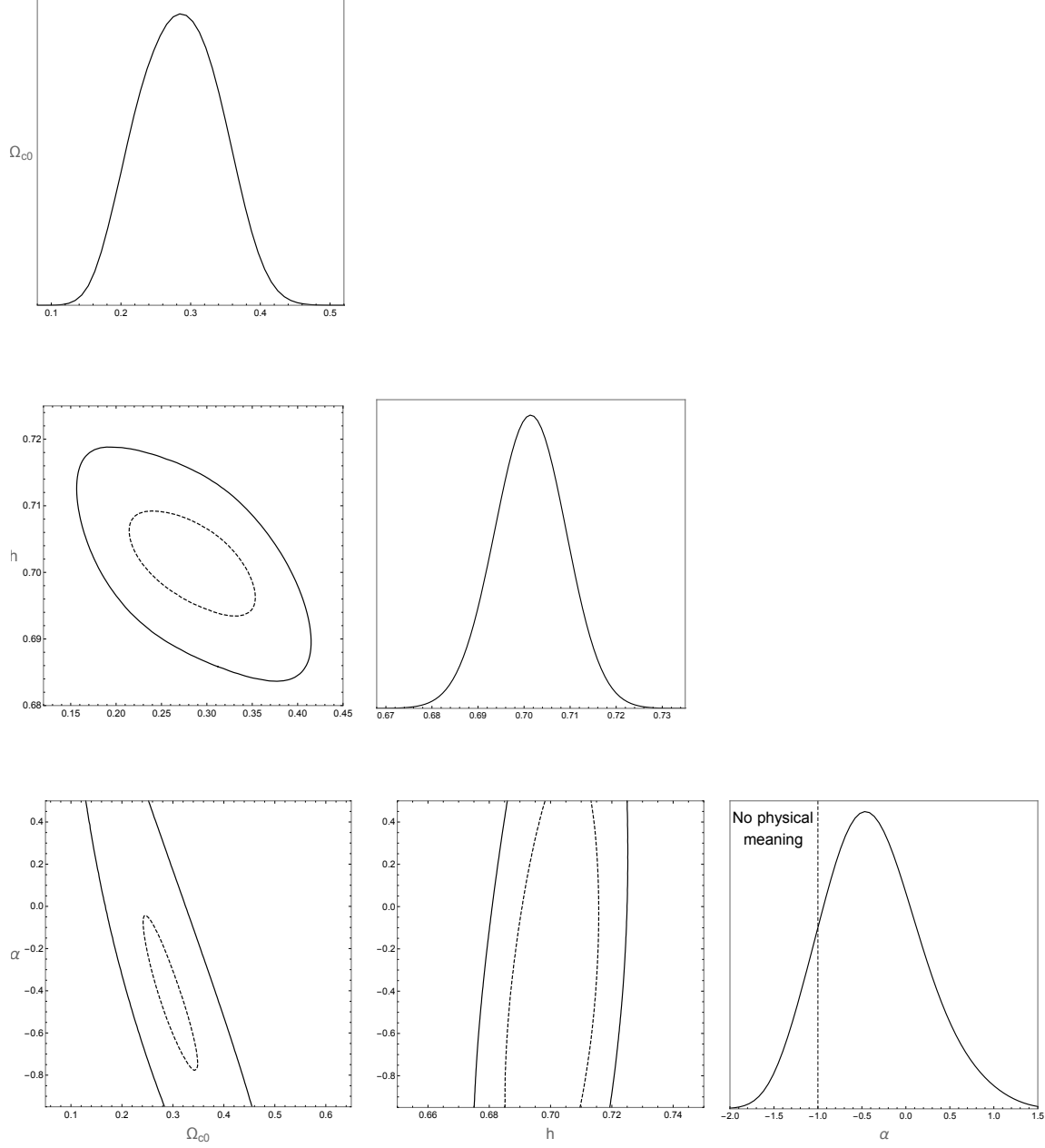


FIG. 3: Marginalized results of SNe Ia statistical analysis for the time-varying vacuum model. Adapting the baryon fractions, this result coincides with the results presented in [20, 43].

Note that, since the dependence on h appears only in H_0 , and the Hubble rate can be written as (14), this deviation depends only on Ω_{c0} and α . Our interest is to find a range in which we can use the approximate solution (26) in the high-redshift regime. Given that the studied model can be seen as a generalization of the Λ CDM model and the parameter that measures the difference to the latter is α , we expect the deviation to be very sensitive to variations in α .

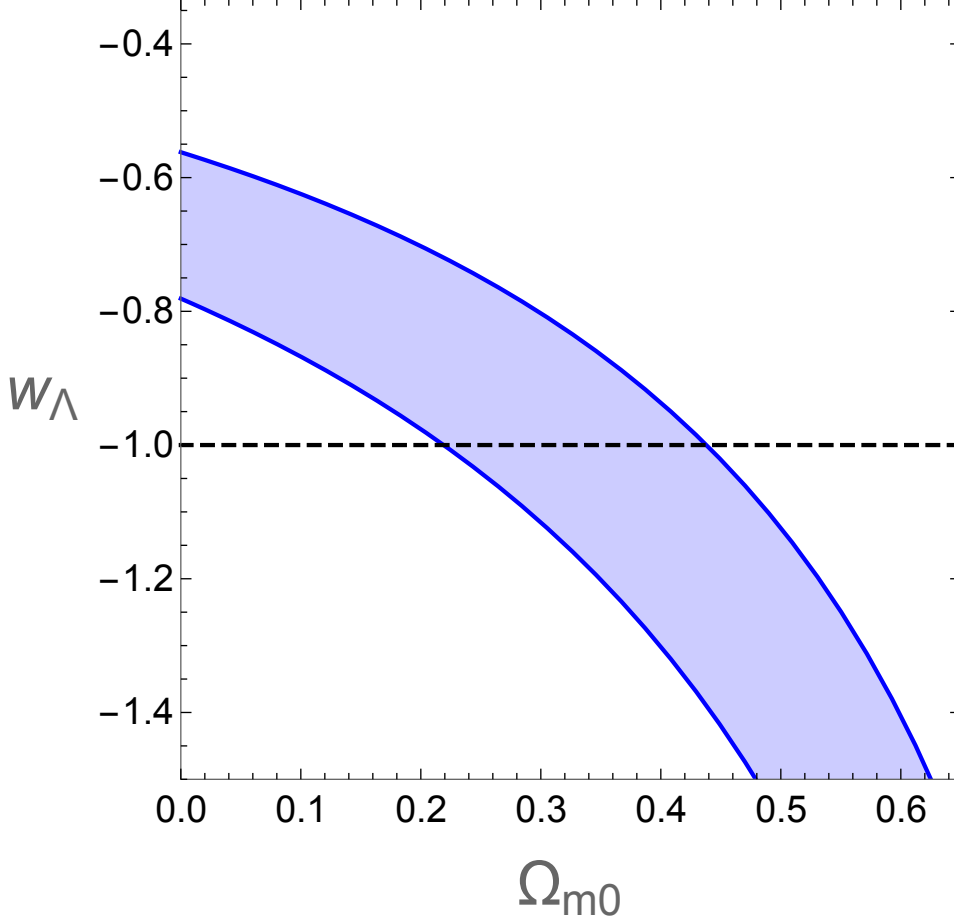


FIG. 4: Region in the $w_\Lambda - \Omega_{m0}$ plane that satisfies the constraint (20), using the 2σ limits for $\tilde{\Omega}_{m0}$ of the SNe Ia statistical analysis.

In order to calculate the deviation we proceed in the following way: first we fix a parameter α within the 2σ interval that was obtained in the SNe Ia analysis. Then we calculate the deviations (31) by using separately the upper and lower limits of the 2σ range for Ω_{c0} (i.e., $0.317 - 0.144$ and $0.317 + 0.078$), found by the SNIa analysis. This results in two curves for (31) in dependence on the scale factor. These curves which confine the error regions for the chosen α are shown in FIG. 5 for several values of α . For all these cases the upper curves correspond to $\Omega_{c0} = 0.317 - 0.144$, the lower ones to $\Omega_{c0} = 0.317 + 0.078$. Increasing α allows us to push the deviation to less than 1%. The results are also summarized in TABLE II. Interestingly, the maximal error of the approximate solution does not occur at the highest redshift but at some intermediate value. For positive values of α the deviation is negligible.

In view of these results for the deviation (31) of the approximate expression (26) from the exact solutions we shall impose from now on the *prior* $\alpha > -0.55$ in order to keep the error

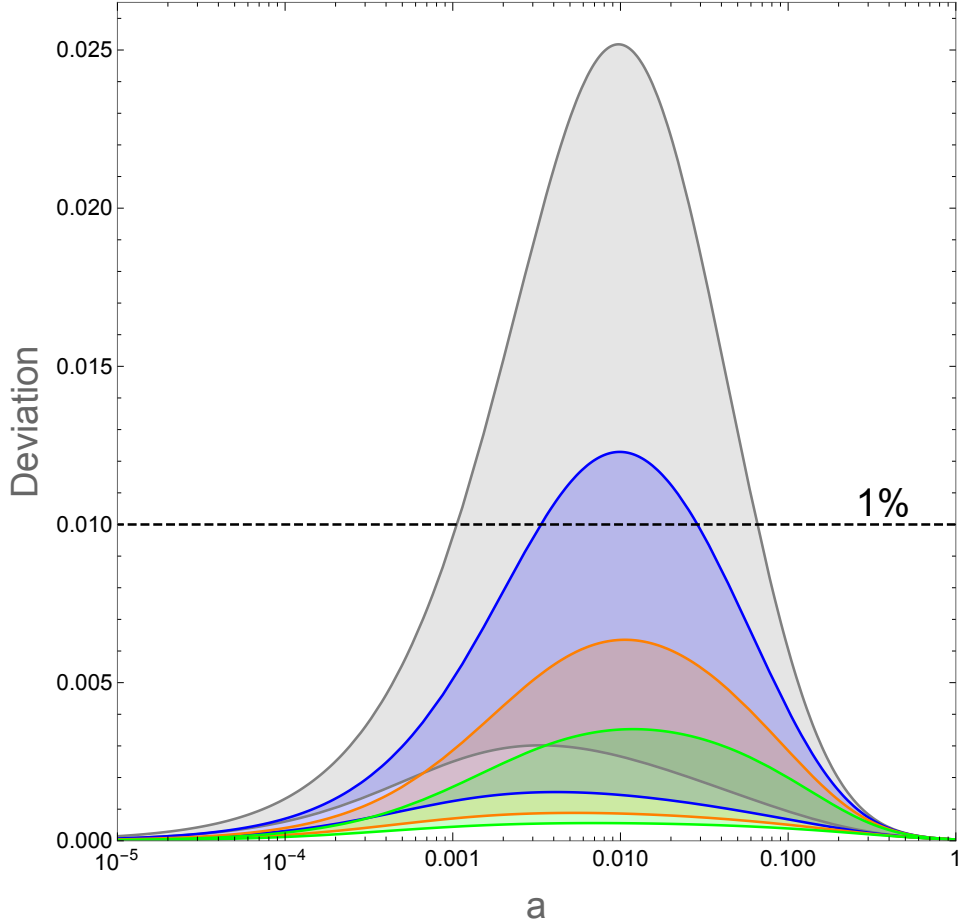


FIG. 5: Deviation between the approximate solution (26) and the numerical solution of (16). Each colored region is associated with a certain value of α . (Gray for $\alpha = -0.65$, blue for $\alpha = -0.60$, orange for $\alpha = -0.55$ and green for $\alpha = -0.50$). All regions are bound by a lower curve, corresponding to the upper 2σ -limit $\Omega_{c0} = 0.317 + 0.078$ and an upper curve for the lower- 2σ limit $\Omega_{c0} = 0.317 - 0.144$.

TABLE II: DEVIATION (31).

Ω_{c0}	α	Maximum deviation
$0.317 \pm_{0.144}^{0.078}$	-0.8	20,0%
	-0.7	5,28%
	-0.6	1,23%
	-0.5	0.353%
	-0.4	0.135%

well below the 1% level.

VI. PERTURBATION DYNAMICS

Restricting ourselves to scalar perturbations in a spatially flat universe, the perturbed Robertson-Walker metric in the Newtonian gauge with the scalar degrees of freedom ψ and ϕ is

$$ds^2 = a^2(\tau) [-(1 + 2\psi) d\tau^2 + (1 - 2\phi) dx^i dx_i]. \quad (32)$$

This metric leads to the set of Einstein's equations [42]

$$k^2\phi + 3\mathcal{H}(\phi' + \mathcal{H}\psi) = -4\pi Ga^2\hat{\rho}, \quad (33)$$

$$\phi' + \mathcal{H}\psi = -4\pi Ga^2\hat{v}, \quad (34)$$

$$\phi'' + \mathcal{H}(\psi' + 2\phi') + (2\mathcal{H}' + \mathcal{H}^2)\psi + \frac{k^2}{3}(\phi - \psi) = \frac{4\pi}{3}Ga^2\hat{p}, \quad (35)$$

$$k^2(\phi - \psi) = 12\pi Ga^2(\rho + p)\hat{\sigma}. \quad (36)$$

Here, the prime denotes the derivative with respect to the conformal time τ and $\mathcal{H} \equiv \frac{a'}{a}$ is the Hubble parameter with respect to the conformal time. The hat denotes first-order variables. The quantity $\hat{\sigma}$ is associated with anisotropic stress perturbations, \hat{v} is the total peculiar velocity potential, related to the spatial components of the four-velocity by $\partial^i \hat{v} = a u^i$.

In order to obtain the CMB and linear matter power spectra we have to solve the complete set of perturbation equations for all components of the universe. The standard procedure to obtain the CMB temperature anisotropies is to compute the Boltzmann equations for all these components. Here we assume that baryons and radiation behave in the same way as they do in the Λ CDM model, i.e., interacting with each other via Thomson scattering before recombination but not directly with the dark sector. Thus, the Boltzmann equations for these two components will be the same as the well-established equations of [42]. However, since we do not have yet a microscopic description of the interaction between the dark components, corresponding Boltzmann equations are not available either. Instead, we have to use the fluid dynamical description for the components of the dark sector.

Generally, a cosmic fluid A with a perfect-fluid energy-momentum tensor

$$T_A^{\mu\nu} = \rho_A u_A^\mu u_A^\nu + p_A h_A^{\mu\nu}, \quad (37)$$

obeys the energy-momentum balance

$$\nabla_\mu T_A^{\mu\nu} = Q_A^\nu, \quad (38)$$

where interactions with other components of the cosmic substratum are included by a source (loss) term Q_A^ν , which can be split according to

$$Q_A^\mu = Q_A u_A^\mu + \hat{F}_A^\mu, \quad \text{where} \quad \hat{F}_A^\mu u_{A\mu} = 0. \quad (39)$$

The crucial quantities for a perturbative analysis are the density contrast δ_A and the peculiar velocity potential \hat{v}_A , which are defined by,

$$\delta_A = \frac{\hat{\rho}_A}{\rho_A}, \quad (40)$$

$$\partial^i \hat{v}_A = a u_A^i, \quad (41)$$

where u_A^i is the four-velocity of component A . If the fluid has a constant EoS parameter w_A , the energy balance takes the form

$$\begin{aligned} \delta'_A + 3\mathcal{H}(c_{sA}^2 - w_A) \delta_A \\ - 9\mathcal{H}^2(1 + w_A)(c_{sA}^2 - w_A) \hat{v}_A - (1 + w_A)(k^2 \hat{v}_A + 3\phi') \\ = a \frac{Q_A}{\rho_A} [\psi - \delta_A - 3\mathcal{H}(c_{sA}^2 - w_A) \hat{v}_A] + a \frac{\hat{Q}_A}{\rho_A}, \end{aligned} \quad (42)$$

where c_{sA}^2 is the comoving sound speed and \hat{Q}_A is the perturbation of the temporal component of the interaction term. Moreover, the general momentum balance is

$$\begin{aligned} \hat{v}'_A + \mathcal{H}(1 - 3c_{sA}^2) \hat{v}_A + \frac{c_{sA}^2}{1 + w_A} \delta_A + \psi \\ = a \frac{Q_A}{\rho_A(1 + w_A)} [\hat{v} - (1 + c_{sA}^2) \hat{v}_A] + \frac{a}{1 + w_A} \frac{\hat{f}_A}{\rho}, \end{aligned} \quad (43)$$

where \hat{f}_A is introduced through

$$\hat{F}_A^i = \frac{1}{a} \partial^i \hat{f}_A. \quad (44)$$

For the case $w_\Lambda = -1$ the DE peculiar velocity potential has no dynamics and the energy balance (42) reduces to,

$$\delta'_\Lambda + 3\mathcal{H}(c_s^2 + 1) \delta_\Lambda = a \frac{Q}{\rho_\Lambda} (\psi - \delta_\Lambda) + \frac{a}{\rho_\Lambda} \hat{Q}, \quad (w_\Lambda = -1), \quad (45)$$

where we dropped the index Λ in Q , i.e. $Q = Q_\Lambda$. Since for $w_\Lambda = -1$ the DE peculiar velocity potential is not a dynamic variable, we can use equation (43) to obtain the spatial perturbation of the interaction term,

$$\hat{f} = \frac{c_s^2 \rho_\Lambda \delta_\Lambda}{a} - Q \hat{v}, \quad (w_\Lambda = -1). \quad (46)$$

For the CDM component the energy and momentum balances are

$$\delta'_c - k^2 \hat{v}_c - 3\phi' = -a \frac{Q}{\rho_c} (\psi - \delta_c) + a \frac{\hat{Q}}{\rho_c}, \quad (w_\Lambda = -1), \quad (47)$$

and

$$\hat{v}'_c + \mathcal{H} \hat{v}_c + \psi = -a \frac{Q}{\rho_c} (\hat{v} - \hat{v}_c) - a \frac{\hat{f}}{\rho_c}, \quad (w_\Lambda = -1), \quad (48)$$

respectively. Note that in the equations above Q is given by equation (11), and \hat{f} is given by equation (46).

The perturbation \hat{Q} of the interaction term has to be chosen on physical grounds. We assume that the expression (8) continues to be valid at first order. One realizes that (8) can covariantly be written as $\rho_\Lambda = \rho_\Lambda \left(\frac{\Theta}{\Theta_0}\right)^{-2\alpha}$, where the expansion scalar $\Theta \equiv u^\mu_{;\mu}$ reduces to $\Theta = 3H$ in the background. Recall that in our four-component model (8) is an ansatz, motivated by the fact that it is an exact relation in a two-component universe of CDM and DE which in total behaves as a generalized Chaplygin gas. This assumption leads to a first-order DE density contrast

$$\delta_\Lambda = -\frac{2\alpha}{3H} \hat{\Theta}, \quad (49)$$

where $\hat{\Theta}$ in the Newtonian gauge is

$$\hat{\Theta} = \frac{1}{a} (\psi' + \phi' - k^2 \hat{v}). \quad (50)$$

The first-order source term is then obtained by introducing (49) in (45) and solving for \hat{Q} .

VII. NUMERICAL COMPUTATION

Now we apply the CLASS code to the set of perturbation equations of the previous section. Since we are looking for a concordance model, we use the 2σ range of α values, obtained from the SNe Ia statistical analysis in section IV. The procedure is as follows: we fix an α value out of the 2σ confidence interval of the SNIa analysis. Then we compute the CMB and matter power spectra using the upper and the lower limits of the 2σ confidence interval for Ω_{c0} . Since these limits depend on α (see the $\Omega_{c0} - \alpha$ contour curves in FIG. 3), we have to choose a slightly different range of Ω_{c0} values for each value of α . TABLE III lists various values of α with the corresponding limits of the 2σ range of Ω_{c0} . In the following subsection we use the values in TABLE III to compute the CMB power spectrum. Afterwards we compare the

TABLE III: Result of SNe Ia statistical analysis for the time varying vacuum model.

α	Ω_{c0} (Minimum)	Ω_{c0} (Maximum)
-0.50	0.238	0.377
-0.25	0.207	0.342
-0.05	0.185	0.316
+0.05	0.174	0.303
+0.25	0.154	0.279

transfer function for our time-varying vacuum model obtained with CLASS with the modified BBKS transfer function proposed in [20, 43]. Finally, we confront the linear matter power spectrum with its Λ CDM counterpart.

A. CMB power spectrum

In this study we use $h = 0.697$ according to TABLE I. The following steps are similar to those already made in the background analysis. For each value of α we calculate the CMB power spectra for the corresponding upper and lower limits of the 2σ interval for Ω_{c0} in TABLE III. Then we compare the resulting plots with the Planck data [41]. The results are shown in FIGs. 6-10. The black solid curves are those for the upper and lower 2σ limits of the Ω_{c0} values, the red solid curve represents the best-fit Planck result for the Λ CDM model. The blue dots are the binned data for the CMB power spectrum from Planck. We will consider a time varying vacuum model competitive if the Planck CMB spectrum (blue dots) lies inside the region which is confined by the two black curves, resulting from the upper and lower limits for Ω_{c0} . Any model for which the blue dots lie outside this region is ruled out. FIG. 6 shows the CMB power spectrum for $\alpha = -0.50$ which can be associated to the model of a cosmological term that decays linearly with the Hubble rate [28, 30, 40]. Although it reproduces well the position of the first acoustic peak, it clearly does not meet our criterion for a competitive cosmological model. There is no concordance between the SNe Ia analysis and the CMB spectrum. This result confirms an earlier analysis in [44] and, for small l , also reproduces the result of [45]. FIG. 7 presents the result for $\alpha = -0.25$. Still, the Planck result is outside the region between the black curves although the difference is somewhat diminished compared with the previous case. In FIGs. 8 and 9, corresponding to $\alpha = -0.05$ and $\alpha = +0.05$ respectively, the Planck result is inside the regions that are confined by the

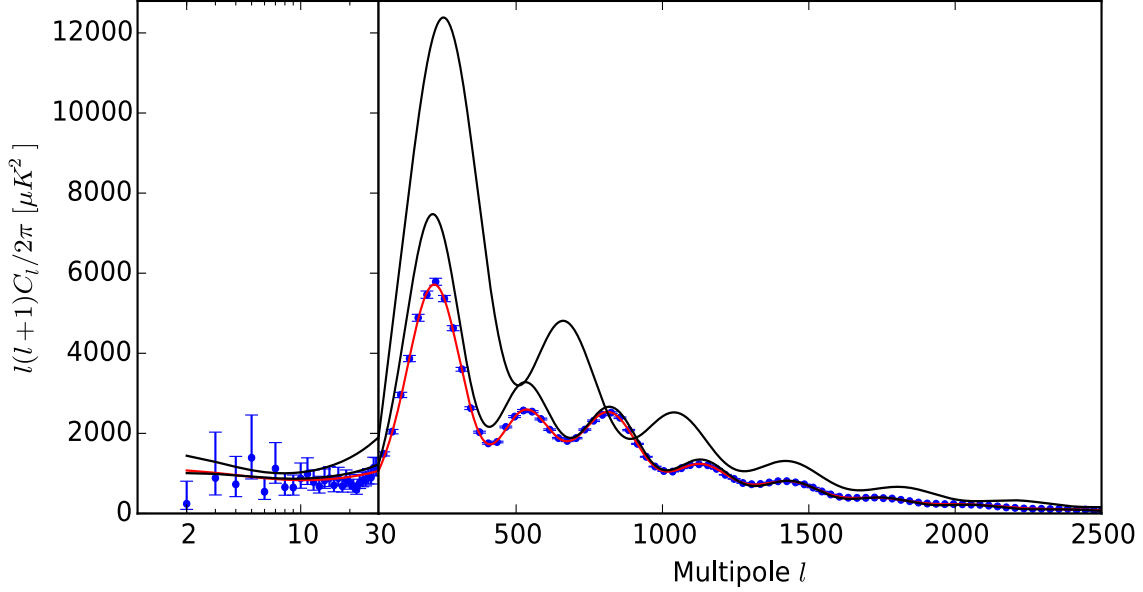


FIG. 6: CMB spectrum for the decaying vacuum model with $\alpha = -0.50$.

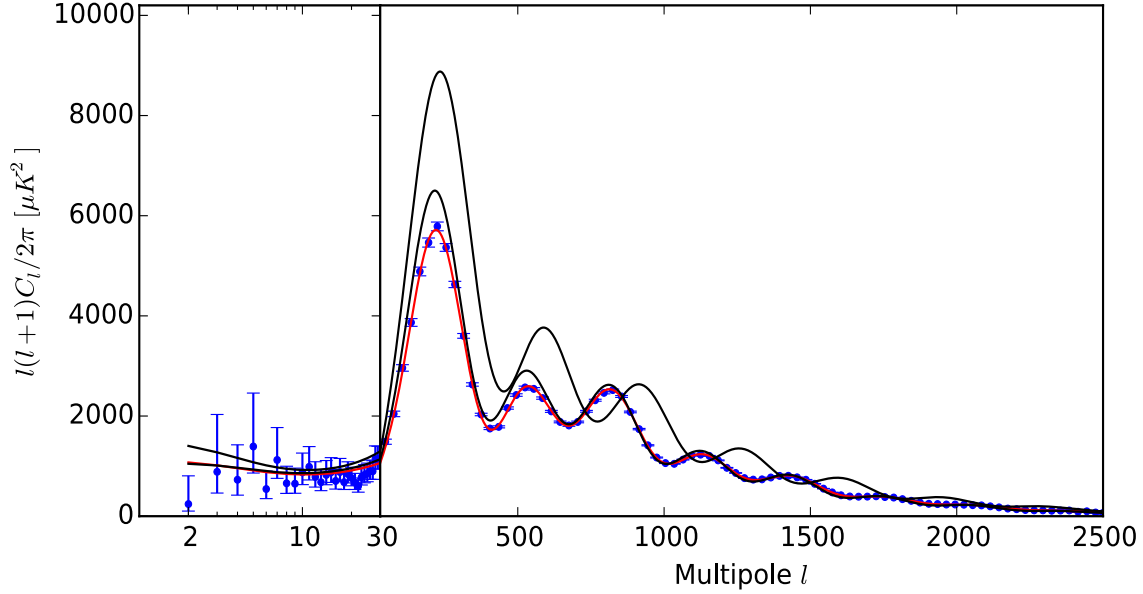


FIG. 7: CMB power spectrum for the decaying vacuum model with $\alpha = -0.25$.

two black curves which mark the upper and lower limits for Ω_{c0} . Anticipating that still larger positive values of α are not favored as well, this means, it is only for $|\alpha| \lesssim 0.05$ that the time varying vacuum models provide a correct CMB spectrum. In other words, these models have to be very close to the Λ CDM model. Recall that a positive α describes an energy transfer from CDM to the vacuum, i.e., a matter decay. The already mentioned result that larger positive values of α do not correctly describe the CMB spectrum is visualized in FIG. 10,

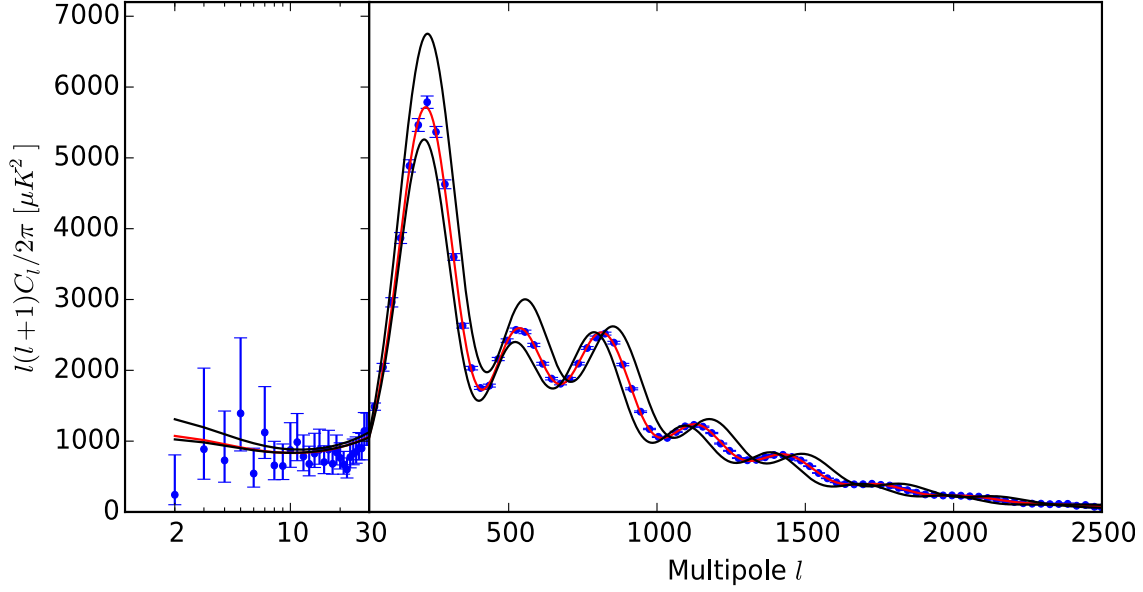


FIG. 8: CMB power spectrum for the decaying vacuum model with $\alpha = -0.05$.

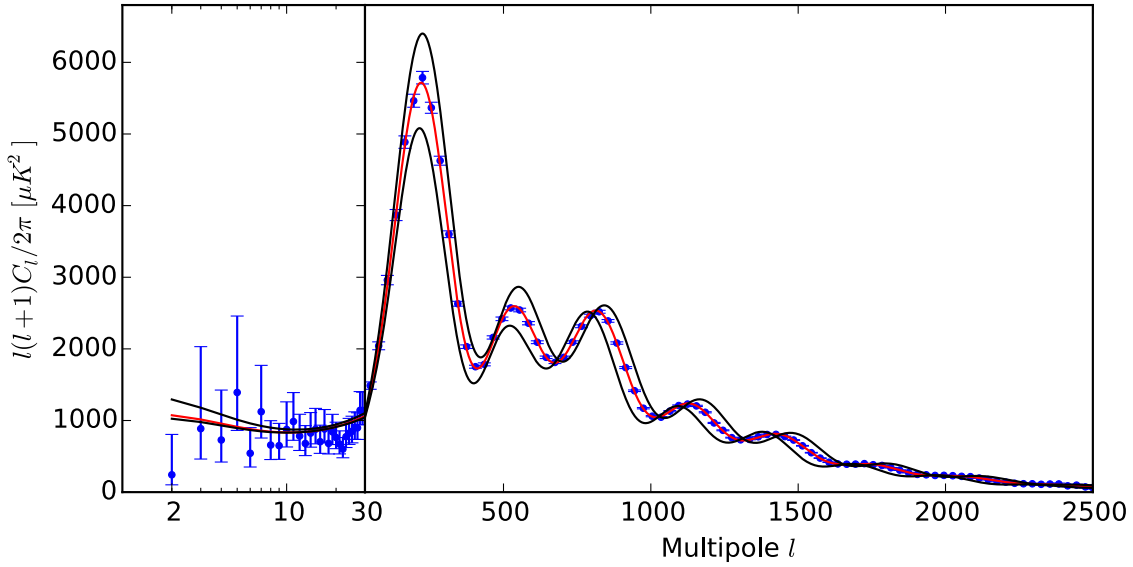


FIG. 9: CMB power spectrum for the decaying CDM model with $\alpha = +0.05$.

where we choose $\alpha = +0.25$. In this case the Planck result is again outside the region confined by the black curves, this time the height of the first peak is too small, whereas it was too large in FIGs. 6 and 7. We recall that positive values of α correspond to an energy flux from the vacuum to CDM.

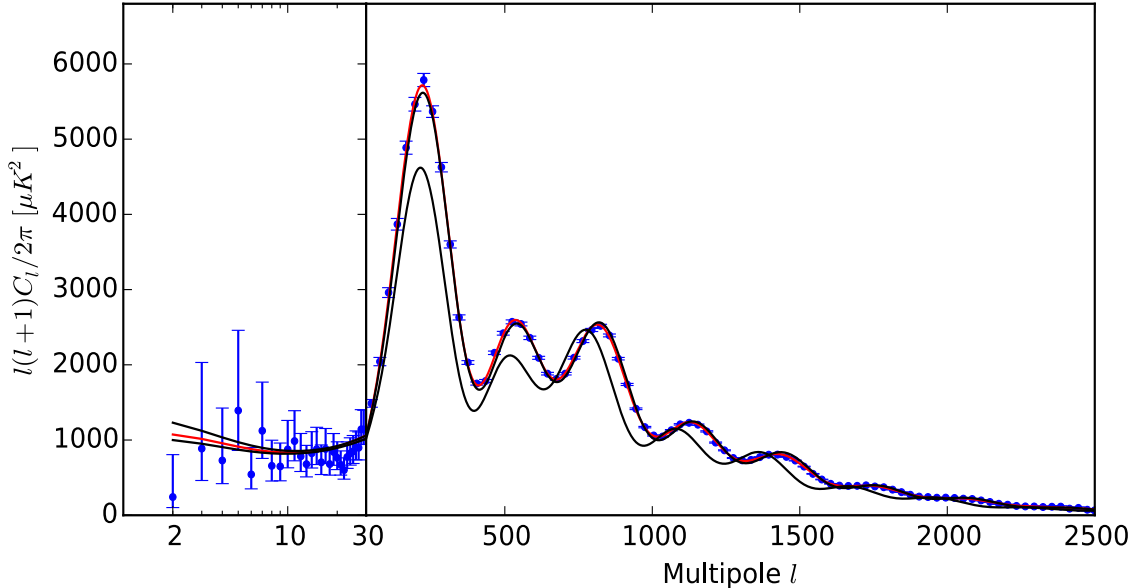


FIG. 10: CMB power spectrum for the decaying CDM model with $\alpha = +0.25$.

B. Transfer function

Here we consider the matter transfer function for the time-varying vacuum model. The transfer function is generally defined as (cf. [46])

$$T(k) \equiv \frac{\delta_m(k, z=0)}{\delta_m(k, z=\infty)} \frac{\delta_m(0, z=0)}{\delta_m(0, z=\infty)}. \quad (51)$$

The widely used BBKS transfer function [47] is known to be a fit formula for the Λ CDM model that depends on k/k_{eq} , where k_{eq} is the comoving horizon scale at the time of matter-radiation equality,

$$T(x = k/k_{eq}) = \frac{\ln(1 + 0.171x)}{(0.171x)} \left[1 + 0.284x + (1.18x)^2 + (0.399)^3 + (0.490x)^4 \right]^{-0.25}. \quad (52)$$

We start by comparing the transfer functions from CLASS [1], from Eisenstein and Hu [46] (EH97) and from [47] (BBKS86) for the Λ CDM model. This is shown in FIG. 11. A different representation of the same curves with a higher resolution and with the inclusion of baryons in the EH97 transfer functions is provided in FIG. 12. Here, $f_b = \frac{\Omega_{b0}}{\Omega_{m0}}$. The differences between the BBKS86 and the EH97 curves are of the order of 5% only if baryons are not included. Otherwise there are substantial deviations. On the other hand, the EH97 transfer function with baryons ($f_b = 0.158$) reproduces the result from CLASS to better than 3% (lower part of the figure). It has been suggested that the linear matter power spectrum of a decaying vacuum model can be obtained using a modified BBKS transfer function [20, 43].

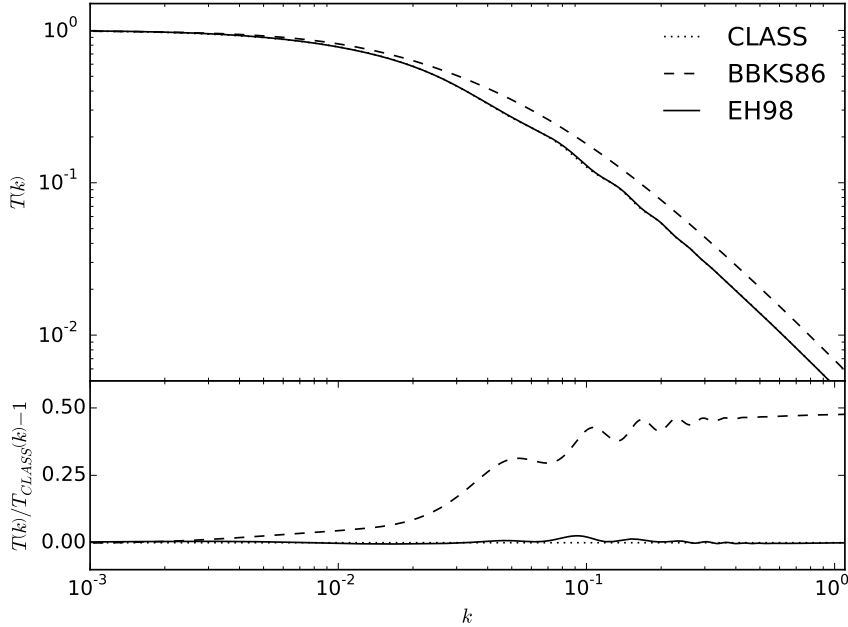


FIG. 11: Transfer functions for the Λ CDM model. BBKS86 refers to [47] and EH97 refers to [46]. The curves EH97 and CLASS are almost indistinguishable in the upper part. The lower part visualizes the departure of the BBKS transfer function from the transfer function from CLASS for $k \gtrsim 10^{-2}$, i.e. still in the linear regime while the curves for CLASS and EH97 almost coincide in the entire range.

The modification is motivated by the fact that matter production will change the time of matter-radiation equality compared with the Λ CDM model. According to [20, 43] this is taken into account by a modification in k_{eq} in (52),

$$k_{eq} = \sqrt{\frac{2}{\Omega_{r0}} \frac{\Omega_{c0}^{1+\alpha}}{l_{H0}}}, \quad (53)$$

where l_{H0} is the present Hubble radius. The Λ CDM value corresponds to $\alpha = 0$. In FIG. 13 we compare this modified BBKS transfer function with the CLASS transfer function for the best-fit values in TABLE I. For comparison we have also included the EH97 transfer function with the modification (53). The modification (53) is indicated by a plus sign. It is obvious that the modified BBKS function is considerably different from its CLASS counterpart for $k \gtrsim 10^{-2}$.

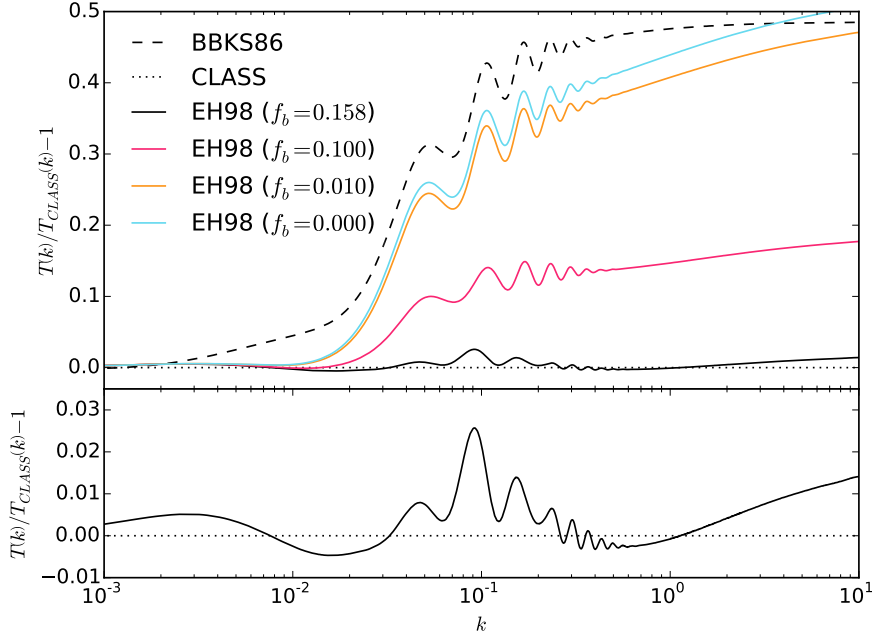


FIG. 12: Transfer functions for the Λ CDM model. The upper part depicts the deviations of the CLASS and of the EH97 transfer functions with different baryon content from BBKS86. The latter is a reasonable approximation (at the 5% level) to EH97 only if baryons are not taken into account. EH97 with $f_b = 0.158$ coincides with CLASS up to 3% (lower part of the figure).

C. Growth rate and linear matter power spectrum

The modified CLASS code also allows us to obtain the growth rate and the linear matter power spectrum for the time-varying vacuum model. The growth rate is defined by $f = \frac{d \ln \delta_m}{d \ln a}$. Both δ_m and f are depicted in FIG. 14 for the values $\alpha = -0.5$, $\alpha = -0.25$, $\alpha = -0.05$, $\alpha = +0.05$ and $\alpha = +0.25$, listed in TABLE III. In FIG. 15 we illustrate the corresponding power spectra for all these cases. The black solid lines are obtained analogously to those of the previous CMB analysis. A chosen α is combined with the upper and lower limits of the admissible range of Ω_{c0} values. The red lines represent the Λ CDM results. Consistent with the results for the CMB spectra, it is only for $\alpha = -0.05$ and $\alpha = +0.05$ that the Λ CDM curves in FIGs. 14 and 15 lie inside the range limited by the combination of α with the admitted values for Ω_{c0} . This double confirmation gives strong support to the conclusion that these types of time-varying vacuum models are strongly constrained. They survive only as long as they stay very close to the standard model.

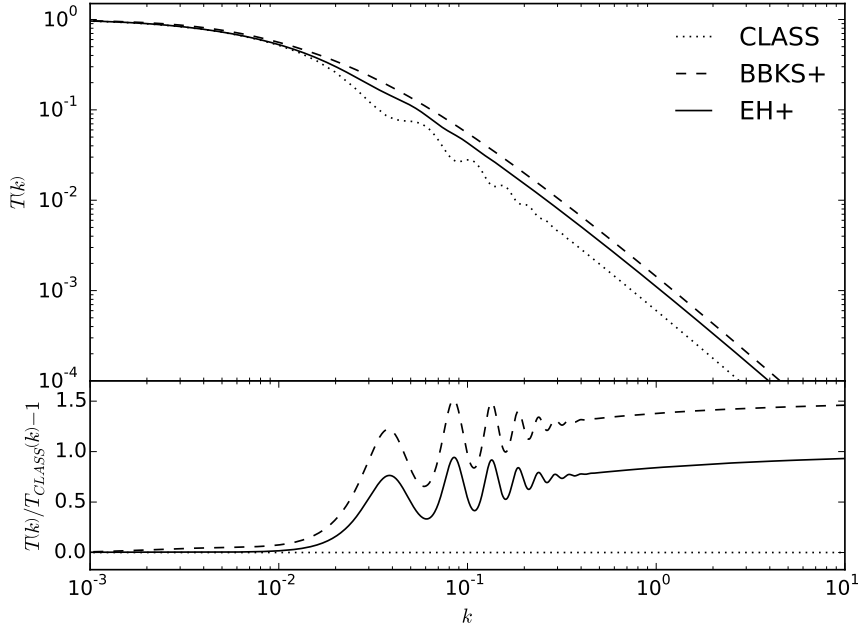


FIG. 13: Transfer functions for the decaying vacuum model with the best-fit values of TABLE I. The plus sign in BBKS+ and EH+ indicates that in the transfer functions [47] (see (52)) and [46] the modification (53) was applied. For any $k \gtrsim 10^{-2}$ this does not result in an acceptable approximation to the result from CLASS.

VIII. CONCLUSIONS

A cosmological dynamics in which the dark sector is modeled as a gCg with an EoS $p = -\frac{A}{\rho\alpha}$ is only compatible with observations if the parameter α is restricted to $|\alpha| \lesssim 0.05$, i.e., it has to be very close to the Λ CDM model which corresponds to $\alpha = 0$. A negative α describes a decaying vacuum, whereas $\alpha > 0$ is equivalent to a decay of dark matter. While the SNIa analysis on the basis of the JLA sample leaves room for a broad range of date including $\alpha = -1$ and $\alpha = 0$ (at the 2σ confidence level), the Planck data for the CMB anisotropy spectrum narrow the admissible interval drastically. The limits obtained from a comparison of the matter power spectrum of the gCg-based model with the corresponding spectrum of the standard model are consistent with $|\alpha| \lesssim 0.05$ as well. We demonstrate that the mere position of the first acoustic peak in the CMB spectrum is not sufficient to assess a cosmological model. In particular, our study is incompatible with a model in which vacuum energy decays linearly with the Hubble rate, corresponding to $\alpha = -\frac{1}{2}$. Further, we

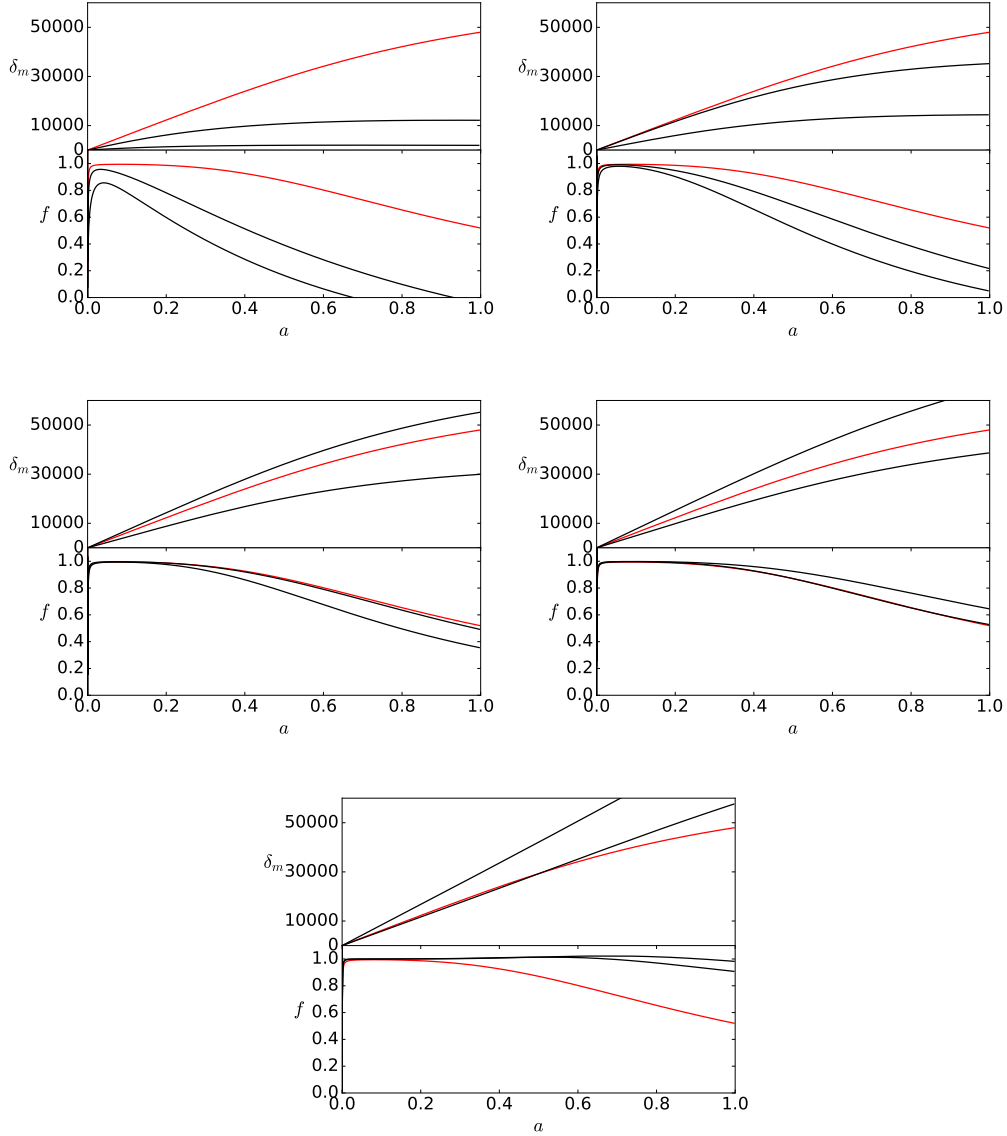


FIG. 14: Matter density contrast δ_m and growth rate f for the parameters of TABLE III. Upper part: $\alpha = -0.5$, $\alpha = -0.25$ (from left to right). Middle: $\alpha = -0.05$, $\alpha = +0.05$. Lower part: $\alpha = +0.25$.

point out that the BBKS matter transfer function does not provide a good approximation to the transfer function of the CLASS code if baryons are taken into account. Modifications of the BBKS expression do not lead to acceptable results. While there remains a small range of admissible α values around zero, our analysis may well be seen as a confirmation of the standard Λ CDM model.

Acknowledgment

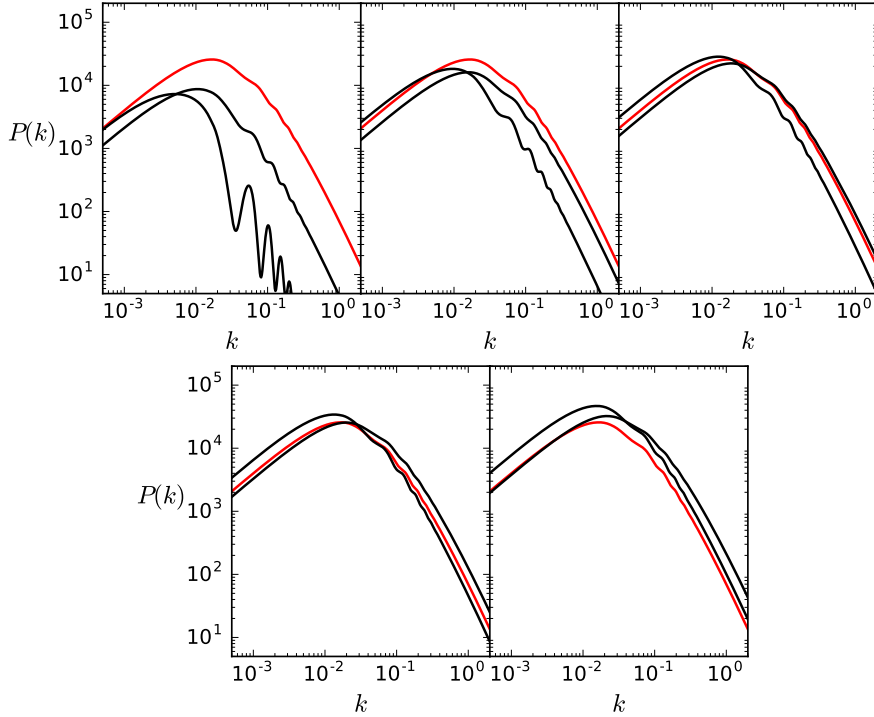


FIG. 15: Linear matter power spectrum for the parameters of TABLE III. Upper part: $\alpha = -0.5$, $\alpha = -0.25$, $\alpha = -0.05$ (from left to right). Lower part: $\alpha = +0.05$ and $\alpha = +0.25$.

Support by CNPq, CAPES and FAPES is gratefully acknowledged. DFM acknowledges the support of the Norwegian Research Council. LC thanks O. Piattella for useful discussions.

-
- [1] D. Blas, J. Lesgourgues, T. Tram, *The Cosmic Linear Anisotropy Solving System (CLASS) II: Approximation schemes*. JCAP **1107**, 034 (2011); arXiv:1104.2933.
 - [2] T. Buchert, A.A. Coley, H. Kleinert, B.F. Roukema and D.L. Wiltshire, *Observational challenges for the standard FLRW model*. Int.J.Mod.Phys. D **25**, 1630007 (2016); arXiv:1512.03313.
 - [3] S. Chaplygin, *On gas jets*. Sci. Mem. Moscow Univ. Math. Phys. **21**, 1 (1904).
 - [4] A.Y. Kamenshchik, U. Moschella and V. Pasquier, *An alternative to quintessence*. Phys. Lett. **B511**, 265(2001).
 - [5] J. C. Fabris, S. V. B. Gonçalves and P. E. de Souza, *Mass Power Spectrum in a Universe Dominated by the Chaplygin Gas*. Gen. Rel. Grav. **34**, 53 (2002)
 - [6] N. Bilic, G. B. Tupper and R. D. Viollier, *Unification of dark matter and dark energy: the inhomogeneous Chaplygin gas*. Phys. Lett. **B535**, 17 (2002).
 - [7] R. Jackiw, *A Particle Field Theorist's Lectures on Supersymmetric, Non-Abelian Fluid Mechanics and d-Branes*. Preprint physics/0010042.

- [8] M.C. Bento, O. Bertolami and A.A. Sen, *Generalized Chaplygin gas, accelerated expansion, and dark-energy-matter unification*. Phys. Rev. **D66**, 043507 (2002).
- [9] V. Gorini, A.Y. Kamenshchik, U. Moschella, O.F. Piattella, A.A. Starobinsky, *Gauge-invariant analysis of perturbations in Chaplygin gas unified models of dark matter and dark energy*. JCAP **0802**, 016 (2008); arXiv:0711.4242.
- [10] O.F. Piattella, *The extreme limit of the generalized Chaplygin gas*. JCAP **1003**, 012 (2010); arXiv:0906.4430.
- [11] J.C. Fabris, S.V.B. Gonçalves, H.E.S. Velten, W. Zimdahl, *Matter Power Spectrum for the Generalized Chaplygin Gas Model: The Newtonian Approach*. Phys.Rev. **D78**, 103523 (2008);arXiv:0810.4308.
- [12] H. Sandvik, M. Tegmark, M. Zaldarriaga and I. Waga, *The end of unified dark matter?*. Phys. Rev. **D69**, 123524 (2004).
- [13] D. F. Mota, J. R. Kristiansen, T. Koivisto and N. E. Groeneboom, Mon. Not. Roy. Astron. Soc. **382**, 793 (2007) doi:10.1111/j.1365-2966.2007.12413.x [arXiv:0708.0830 [astro-ph]].
- [14] R. R. R. Reis, I. Waga, M. O. Calvao and S. E. Joras, *Entropy perturbations in quartessence Chaplygin models*. Phys. Rev. **D68**, 061302 (2003).
- [15] W.S. Hipólito-Ricaldi, H. E. S. Velten and W. Zimdahl, *Non-adiabatic dark fluid cosmology*. JCAP **0906** 016 (2009).
- [16] W.S. Hipólito-Ricaldi, H. E. S. Velten and W. Zimdahl, *Viscous dark fluid Universe: a unified model of the dark sector?*. Phys. Rev. **D82**, 063507 (2010).
- [17] J.C. Fabris, H.E.S. Velten, W. Zimdahl, *Matter power spectrum for the generalized Chaplygin gas model: The relativistic case*. Phys.Rev. **D81**, 087303 (2010); arXiv:1001.4101.
- [18] H.A. Borges, S. Carneiro, J. C. Fabris, W. Zimdahl, *Non-adiabatic Chaplygin gas*. Phys. Lett. **B727**, 37 (2013)
- [19] Y. Wang, D. Wands, L. Xu, J. De-Santiago, and A. Hojjati, *Cosmological constraints on a decomposed Chaplygin gas*. Phys. Rev. **D87**, 083503 (2013)
- [20] S. Carneiro and C. Pigozzo, *Observational tests of non-adiabatic Chaplygin gas*. JCAP **1410**, 060 (2014); arXiv:1407.7812
- [21] M. Özer and M.O. Taha, *A possible solution to the main cosmological problems*. Phys.Lett. **B171**, 363 (1986).
- [22] M. Özer and M.O. Taha, *A model of the universe free of cosmological problems*. Nucl.Phys. **B287**, 776 (1987).
- [23] S. Hervik, D. F. Mota and M. Thorsrud, JHEP **1111**, 146 (2011) doi:10.1007/JHEP11(2011)146 [arXiv:1109.3456 [gr-qc]].
- [24] O. Bertolami, *Time-dependent cosmological term*. Nuovo Cimento Soc. Ital. Fis. **B93**, 36 (1986).
- [25] K. Freese, F.C. Adams, J.A. Frieman and E. Mottola, *Cosmology with decaying vacuum energy*. Nucl. Phys. **B287**, 797 (1987).

- [26] Peng Wang and Xin-He Meng, *Can vacuum decay in our universe?*. *Class. Quant. Grav.* **22**, 283 (2005); arXiv:astro-ph/0408495.
- [27] B. Wang, Y. Gong and E. Abdalla, *Transition of the dark energy equation of state in an interacting holographic dark energy model*. *Phys. Lett.* **B624**, 141 (2005); hep-th/0506069.
- [28] H.A. Borges and S. Carneiro, *Friedmann cosmology with decaying vacuum density*. *Gen. Rel. Grav.* **37**, 1385 (2005); gr-qc/0503037.
- [29] W. Zimdahl, H.A. Borges, S. Carneiro, J.C. Fabris and W.S. Hipolito-Ricaldi, *Non-adiabatic perturbations in decaying vacuum cosmology*. *JCAP* **1104**, 028 (2011).
- [30] R.F. vom Marttens, W.S. Hipólito-Ricaldi, W. Zimdahl, *Baryonic matter perturbations in decaying vacuum cosmology*. *JCAP* **1408** (2014) 004.
- [31] A. Romero Fuño, W.S. Hipólito-Ricaldi, W. Zimdahl, *Matter perturbations in scaling cosmology*. *MNRAS* **457**, 2958 (2016); arXiv:1409.7706.
- [32] R.F. vom Marttens, L. Casarini, W.S. Hipólito-Ricaldi and W. Zimdahl, *CMB and matter power spectra with non-linear dark-sector interactions*. arXiv:1610.01665.
- [33] M. Betoule et al., *Improved cosmological constraints from a joint analysis of the SDSS-II and SNLS supernova samples*. *Astron. Astrophys.* **568** 22 (2014).
- [34] L.L. Honorez, B.A. Reid, O. Mena, L. Verde and R. Jimenez, *Coupled dark matter-dark energy in light of near Universe observations*. *JCAP* **1009**, 029 (2010), arXiv:1006.0877.
- [35] V. Salvatelli, A. Marchini, L. Lopez-Honorez and O.Mena, *New constraints on Coupled Dark Energy from the Planck satellite experiment*, *Phys. Rev.* **D88**, 023531 (2013); arXiv:1304.7119.
- [36] Timothy Clemson, Kazuya Koyama, Gong-Bo Zhao, Roy Maartens and Jussi Väliiviita, *Interacting dark energy: Constraints and degeneracies*, *Phys. Rev.* **D85**, 043007 (2012); arXiv:1109.6234.
- [37] A.A. Costa, Xiao-Dong Xu, Bin Wang and E. Abdalla, *Constraints on interacting dark energy models from Planck 2015 and redshift-space distortion data*, arXiv:1605.04138.
- [38] M. Bouhmadi-López, J. Morais, and A. Zhuk, *The late Universe with non-linear interaction in the dark sector: the coincidence problem*, *Phys.Dark Univ.* **14**, 11 (2016); arXiv:1603.06983.
- [39] Lu Feng, Xin Zhang, *Revisit of the interacting holographic dark energy model after Planck 2015*, arXiv:1607.05567.
- [40] S. Carneiro, C. Pigozzo, H. A. Borges, J. S. Alcaniz. *Phys. Rev.* **D74**, 023532, (2006).
- [41] N. Aghanim et al. [Planck Collaboration: P. A. R. Ade], arXiv:1502.01589 (2015).
- [42] Chung-Pei Ma, E. Bertschinger. *Astrophys. J.* **455** , 7 (1995).
- [43] C. Pigozzo, S. Carneiro, J.S. Alcaniz, H.A. Borges and J.C.Fabris, *Evidence for cosmological particle creation?* *JCAP* **1605**, 022 (2016); arXiv:1510.01794.
- [44] Lixin Xu, Yuting Wang, Hyerim Noh, *Phys.Rev.* **D84**, 123004(2011).
- [45] H. Velten, H. A. Borges, S. Carneiro, R. Fazolo, S. Gomes. *MNRAS* **452** (2015) 2220-2224.
- [46] D.J. Eisenstein and W.Hu, *Baryonic Features in the Matter Transfer Function*, *Astrophys.J.* **496**, 605 (1998); arXiv:astro-ph/9709112.

[47] J.M. Bardeen, J.R. Bond, N. Kaiser and A.S. Szalay, 1986, ApJ. **304**, 15 (1986).